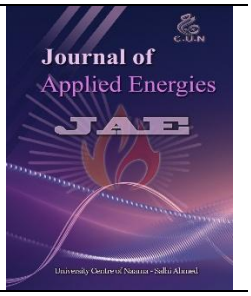
Journal of Applied Energies 01 (2022) 1-10

Journal of Applied Energies



Perforation space impact on the heat dissipation performance in pin fins heat sinks

Djamel Sahel

Technical Sciences Departement, Amar Telidji University of Lagouat, Laghouat, 03000, Algeria.
LCGE laboratory, University of Sciences and Technology, USTO-MB, Oran, Algeria.
Correspondence. Email Address: d.sahel@lagh-univ.dz, djamel_sahel@ymail.com

Abstract: In this study, a numerical analysis is carried out to optimize the pin fins heat sink (PFHS) performance. The investigation is conducted by using Comsol Multiphysics v.5.4 software based on the finite elements method (FEM). The effect of the perforation space through the pin fins is tested. Five configurations are proposed for investigation: cylindrical pin fins (CPFs) and PFHS-1 to 4. The fluid flow and convective heat transfer characteristics are analyzed for Reynolds number (*Re*) ranging from 8,547 to 21,367. The results found that PFHS-1 creates an enhanced heat transfer execution with a moderate pressure drop. In addition, this case ensures the highest hydrothermal performance factor of 1.34. The comparison is reported for CPFs available in the literature, where a satisfactory agreement is observed.

Keywords: Heat sink; Heat dissipation; Pin fins; Perforation; Performance.

1. INTRODUCTION

The rapid development of high-power electronic devices generates another challenge that poses the problem of heating due to the Joule effect, which forces us to reduce or remove

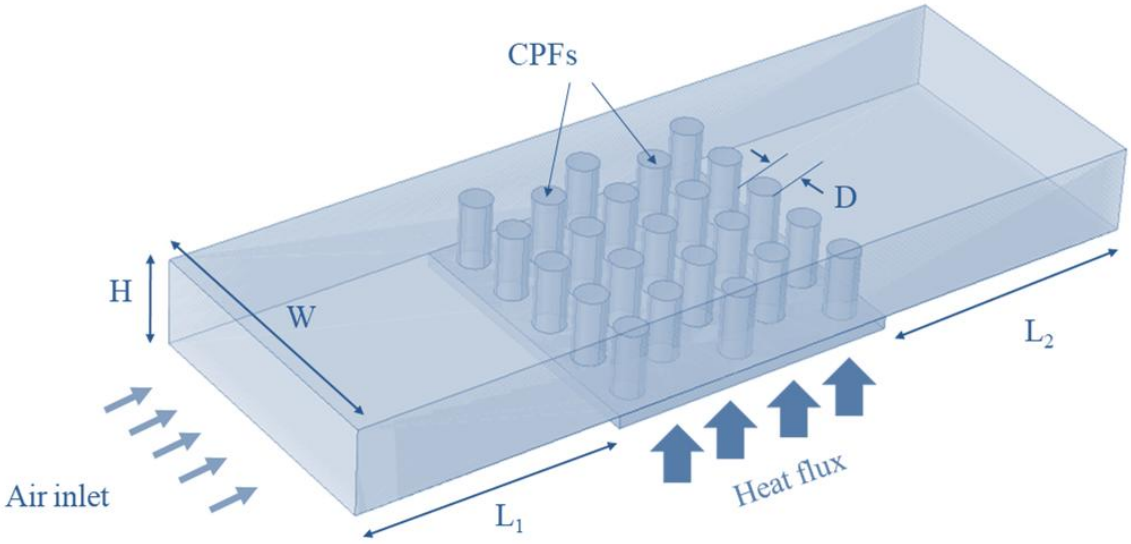
unwanted heat to maintain the normal function of these devices, not to mention the shape and the volumetric design that gets smaller. These challenges have motivated experts to find new techniques to increase the efficiency of the cooling system of such equipment to keep pace with this technological development.

The design strategy of the heat sink is based on the rise of the heat dissipation coefficient and reducing the pressure loss. One of the most reliable methods applied to heat sink designs [1-3] is the insertion of aligned/staggered pin fins over the heated surface to be cooled. In this field, several works have been carried out to study the influence of pin arrangements on thermal performance. Ozsipahi et al. [4] numerically analyzed the hydrothermal performance of an aluminum honeycomb fin heat sink. They tested several geometric and physical parameters such as the height of the fins (H), the distance between fins, and the Reynolds number (*Re*). They reported that the thermal resistance of the honeycomb heat sink (R_{th}) decreases with rising of the fin height. In addition, the heat transfer coefficient and pressure drop increase with the increasing Reynolds number. Haghighi et al. [5] examined the thermal performance of lamellar heat sinks and cubic fin heat sinks. They tested the natural convection regime for a Rayleigh number varying from 8×10^6 to 9, 5×10^6. They concluded that the most significant heat sink layout was seen in the plate cubic pin fin with 7-8 inch and 8.5mm spacing.

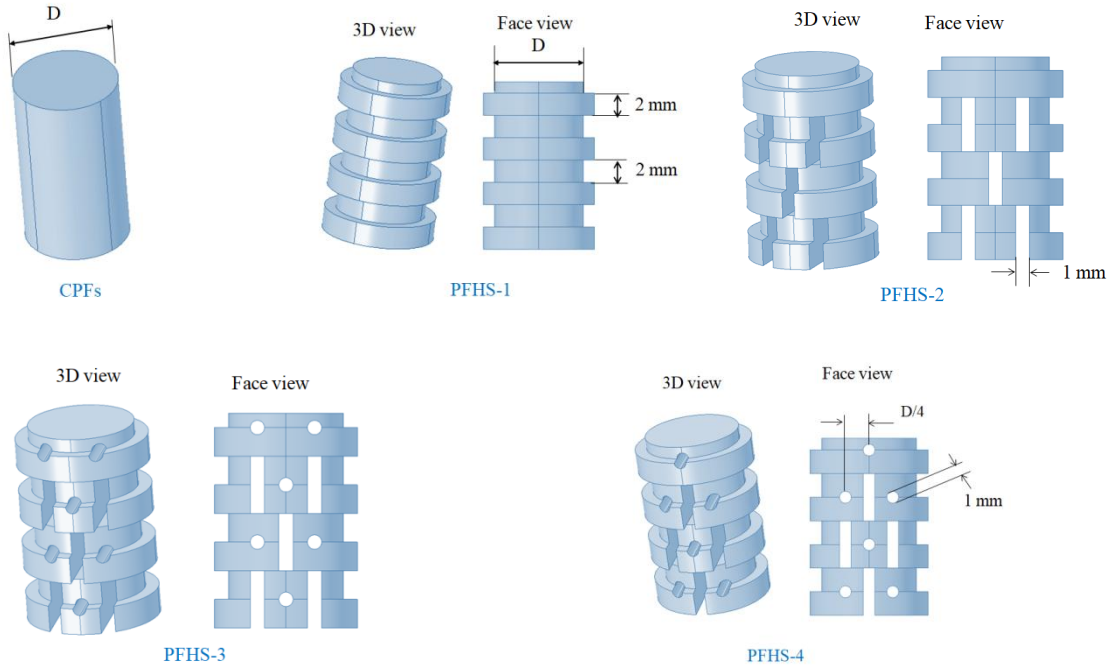
However, the establishment of pockets / hot spots in the downstream zone of the fin is due to the formation of low-speed recirculation zones [6]. For this purpose, perforated pin fins can reduce these areas by mixing the stagnant flow. Meinders et al. [7] reported that the local heat dissipation coefficient could be affected by the size of the recirculation areas behind the pins. Also, Sara et al. [8] concluded that the perforated pin fins could improve performance. Huang et al. [9] numerically estimated the optimal perforation diameter in PFHS. They have shown that perforated fins create a lower pressure drop than those solid fins. Chin et al. [10] conducted an experimental and numerical study to investigate the effect of the number of perforations and the diameter of the perforations in a staggered arrangement. The author demonstrated that the Nusselt number for perforated pins improved by 45% over solid when the number of perforations was higher. In addition, the pressure drop with punched pins is also reduced by 18% compared to solid pins. However, heat dissipation significantly decreases when the pin diameter ratio exceeds 0.375.

In addition, the insertion of the vortex generators (VGs) in the flow direction can considerably enhance the heat dissipation or convective heat transfer execution in the thermal systems [11-13].

In this paper, a numerical investigation was conducted to analyze the effect of some configurations (grooved and perforated pin fins) on the heat transfer and fluid flow characteristics of heat sinks (HSs). For turbulent airflow regime, the investigation was realized by using CFD-Multiphysics COMSOL v.5.4 software. As a consequence, promising results were found to design heat sinks in the future.



a) Configuration of channel heat sinks



b) Different shapes of pin fins

Figure 1: Configuration of, *a)* channel heat sink and b) pin fins.

2. CONFIGURATIONS DESCRIPTION

In this study, the aluminum A5083P type was used to construct the finned heat sinks for different geometries. The different heat sink configurations represent fins placed on the base plate having dimensions W × L_b × e (75×75×4 mm^3). These geometries are located inside the channel, so that the zones located before and after the studied arrangement make it possible to develop flows and to avoid the reversed flow phenomenon. Five arrangements have been studied in this work named as CPFs (*cylindrical pin fins*), and PFHS-1 to 4. The section of the cylindrical fins is characterized by the diameter (D) and the pin fins height (H_P = 15 mm), as shown in Fig. 1. The longitudinal ratio (S_L / H_P) is defined as follows: the ratio between the length of the fins pitch (distance between the centers of fins, where S_L is the height of the fins (H_P), and it is fixed at 1. In addition, all dimensions of the PFHSs are illustrated in the figure.

3. NUMERICAL AND MATHEMATICAL MODELS

The heat transfer and fluid flow characteristics through HSs were numerically examined by using COMSOL v.5.4 software. No isothermal flow interface was utilized to simulate the conjugate heat transfer and fluid flow. The heat transfer by conduction was put through the solid-Aluminum, where the heat transfers by convection implanted by solid-Aluminum/airflow contact.

3.1 Governing equations

The turbulent air flow enters at 300 K, for *Re* changing from 8,547 to 21,367. The governing equations for steady-state and incompressible fluid flow are determined as follows:

Continuity equation

$$\frac{\partial u_i}{\partial x_i} = 0 \tag{1}$$

Momentum Equation

$$\frac{\partial (u_i u_j)}{\partial x_j} = -\frac{\partial \overline{p}}{\partial x_i} + \nu \nabla^2 u_i + \frac{\partial}{\partial x_j}\left(-\overline{u_i' u_j'}\right) \tag{2}$$

Energy Equation

$$\frac{\partial (u_j T)}{\partial x_j} = \alpha \nabla^2 T + \frac{\partial}{\partial x_j}\left(-\overline{u_i' \theta}\right) \tag{3}$$

Heat conduction equation

$$\nabla\left(\lambda_s \nabla T_s\right) = 0 \tag{4}$$

For the closing of the equations system, the RANS-based k-ε turbulence model is used in this paper as a robust model which is primarily utilized for some industrial applications.

3.2 Governing parameters

The governing parameters used in this paper are summarized as follow:

Nusselt number (*Nu*)

$$Nu = \frac{\varphi\, D_h}{\lambda_{air}\left(T_w - (T_{in} - T_{out})/2\right)} \tag{5}$$

Thermal resistance (R_{th})

$$R_{th} = (T_w - T_{in})/\varphi \tag{6}$$

Pressure drop (Δp)

$$\Delta p = p_{in} - p_{out} \tag{7}$$

Hydro thermal performance factor (η)

$$\eta = \frac{\left(Nu / Nu_{CPFS}\right)}{\left(\Delta p / \Delta p_{CPFS}\right)} \tag{8}$$

Reynolds number *(Re*)

$$Re = \frac{U_{in}\, D_h}{\nu} \tag{9}$$

where, D_h is the hydraulic diameter and determined as:

$$D_h = \frac{4 \times A_c}{P} \tag{10}$$

where, P and A_c are the perimeter and cross section of channel, respectively.

The mesh sensibility, its type and number present the main task in the accuracy of the numerical results. For this purpose, the Nusselt number results were obtained by using generated tetrahedral meshes. Different numbers of elements were compared with each other to find established results. So, for all configurations, the definitive grids are: 998, 707, 1,005,433, 1,115,451, 1,128,794 and 1,006,754 for CPFs and PFHS-1 to 4, respectively.

4. RESULTS AND DISCUSSION

4.1 Validation of results

For the comparison and in objective to validate the consistency of the present numerical model, we utilized on the experimental data of Chin et al. [10]. For this interest, the Nusselt number results were used as shown in Figure 2. From this figure, a satisfactory agreement was found.

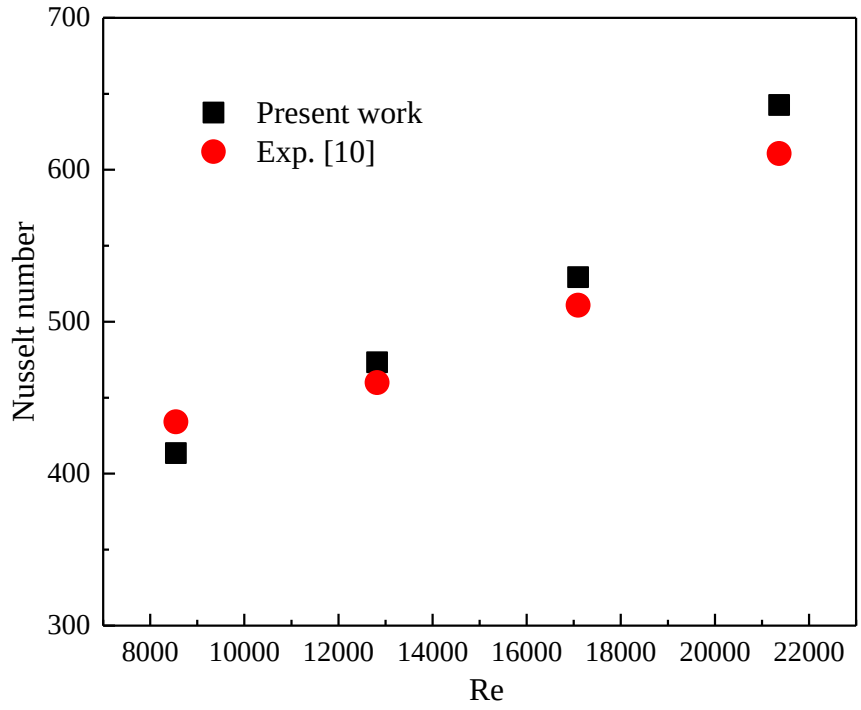


Figure 2: Validation of Nusselt number results.

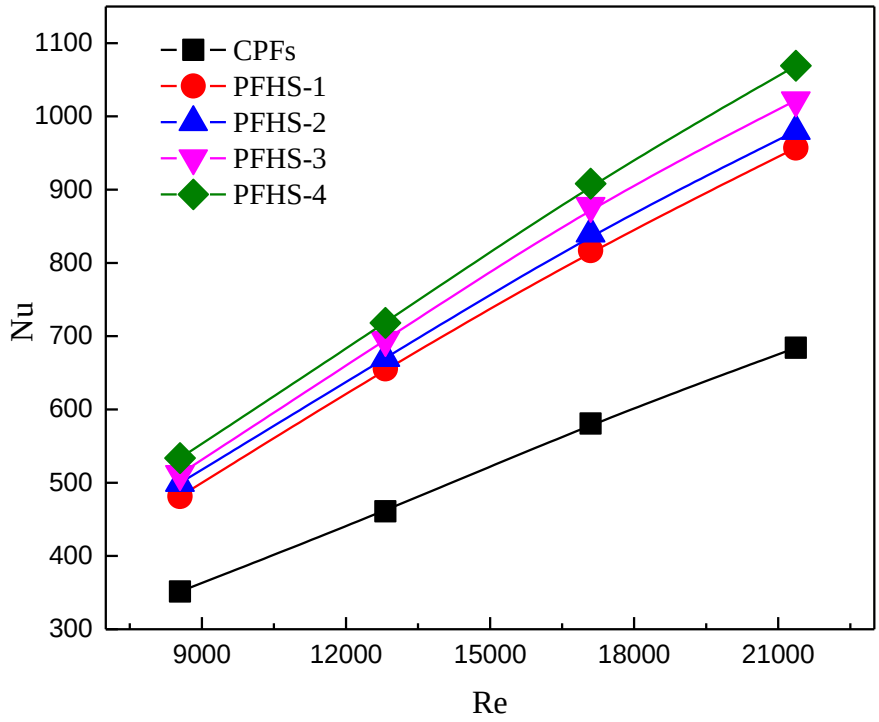


Figure 3: Variation of *Nu* versus *Re*.

4.2 Nusselt number and thermal resistance

Figure 3 presents the variation of Nusselt number versus Reynolds number for all configurations. As shown in the figure, Nusselt number increases with Reynolds number increasing due to the rise of the turbulence intensity. Also, the Nusselt number increased by 40.89%, 44.12%, 50.29% and 57.21% for PFHS-1 to 4 compared with cylindrical pin fins (CPFs) at *Re* = 21,367, respectively. These augmentations are due to the better swirling of fluid flow through the perforation space.

These configurations are also affecting the thermal resistance. Figure 4 depicts the variation of the thermal resistance according to Reynolds number for all arrangements. It can see that the thermal resistance decreases with Reynolds number rising. In addition, the insertion of the perforation space reduces the thermal resistance due to the augmentation of the total heat transfer area. The thermal resistance is decreased by 31.58%, 36.19% 40.76% and 43.88% for PFHS-1 to 4 compared with cylindrical pin fins (CPFs) at *Re* = 21,367, respectively. Consequently, PFHS-4 presents the best performance in terms of heat dissipation within the heat sinks.

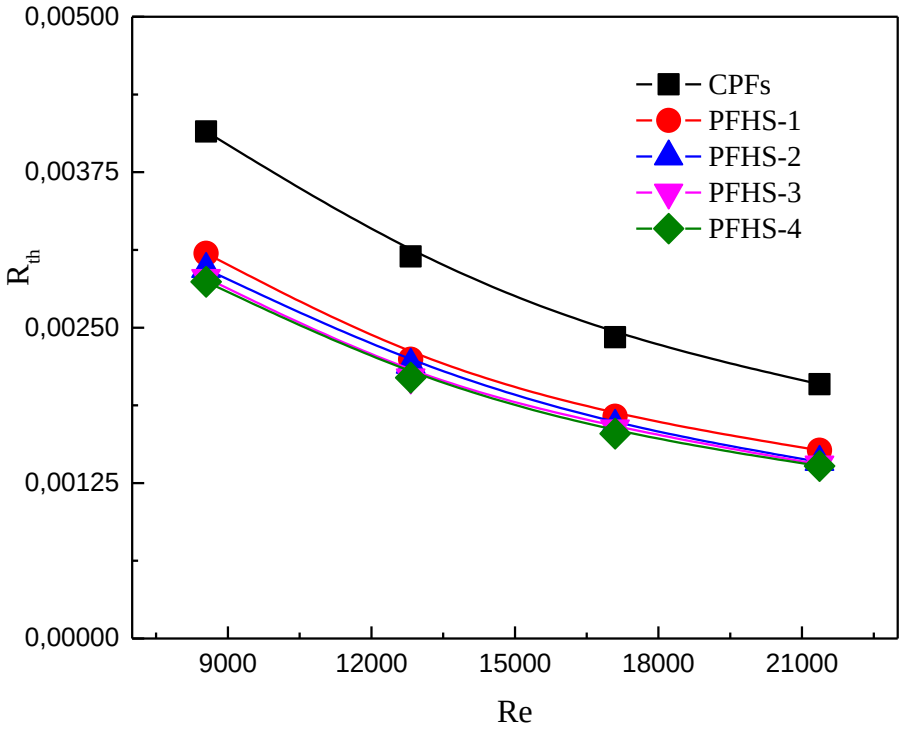


Figure 4: Variation of R_{th} versus *Re*.

4.3 Pressure drop

As with each energetic system, augmentation of heat transfer execution generates the pressure drop penalty. The variation of the pressure drop versus Reynolds number for various geometries is shown in Figure 5. It is clear to see that the pressure drop increases with increasing Reynolds number due to the flow blockage phenomena. Fortunately, a moderate pressure drop is observed as a maximum value for PFHS-4 by 17.40%, at *Re* = 21,367 compared with CPFs.

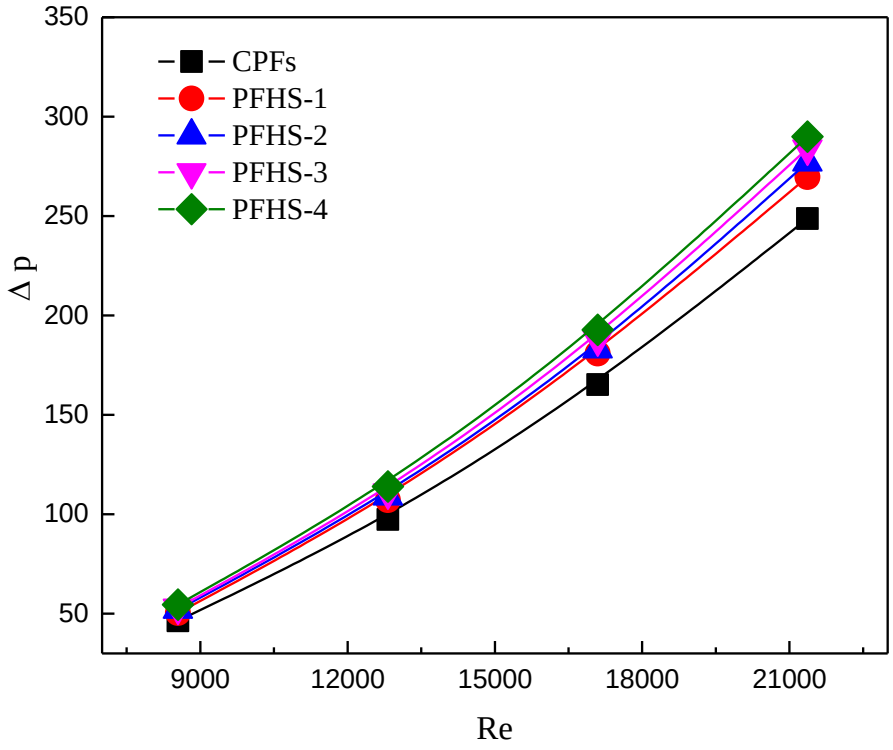


Figure 5: Variation of *Δp* versus *Re*.

4.4 Performance evaluation and optimization

To select the best configuration, the hydrothermal performance factor (η) was determined for all cases. Figure 6 illustrates the variation of hydrothermal performance factor (η) versus Reynolds number. Auspiciously, the η is higher than the unit for all configurations, where the PFHS-4 ensures the highest hydrothermal performance factor of 1.34. So, from this discussion, PFHS-4 merits to be considered in the heat sink design.

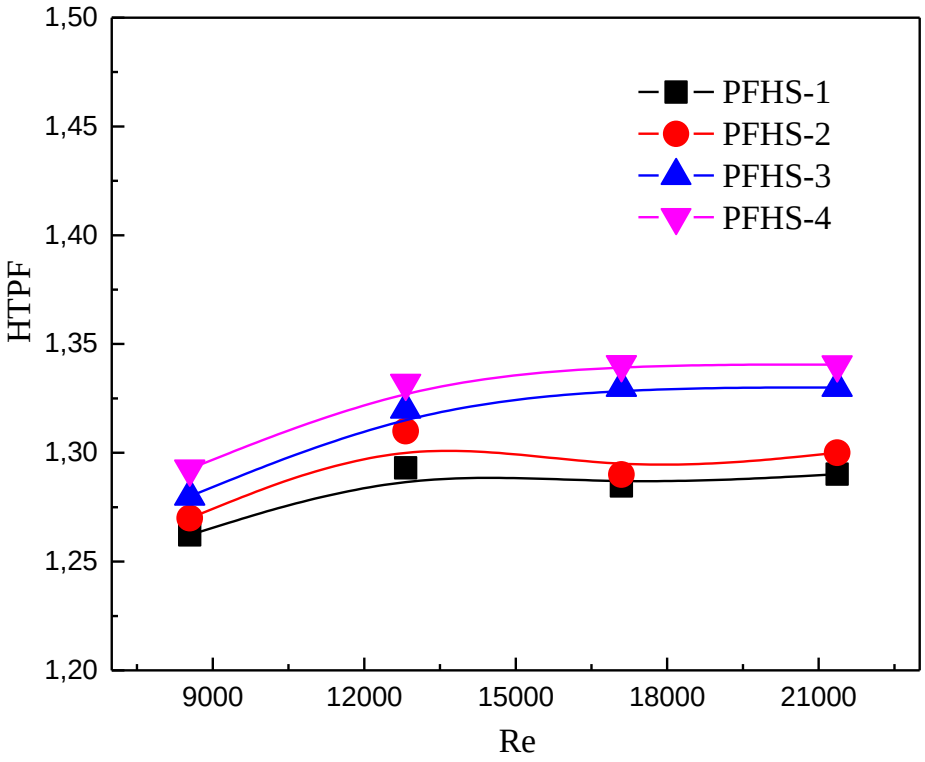


Figure 6: Variation of HTPF versus *Re*.

5. CONCLUSION

The effect of the perforation space on the heat transfer and fluid flow characteristics through the pin fin heat sink were analyzed in this paper. Different forms of perforation space were tested for Reynolds numbers ranging from 8,547 to 21,367. Five geometries were proposed, namely: CPFs (a reference case) and PFHS-1 to 4. The results showed that for PFHS-4, the heat transfer coefficient was augmented by 43.88% compared with CPFs. This augmentation was accompanied by a moderate pressure drop of 17.40%. In addition, the PFHS-4 ensured the highest hydrothermal performance factor (η) of 1.34. This case was selected as a recovered configuration for the heat sink design.

REFERENCES

[1] Sahel, D., Bellahcene, L., Yousfi, A., Subasi, A. (2021). Numerical investigation and optimization of a heat sink having hemispherical pin fins. *International Communications in Heat and Mass Transfer*, 122, 105133.

[2] Yousfi, A., Sahel, D., Mellal, M. (2019). Effects of a pyramidal pin fins on CPU heat sink performances. *Journal of Advanced Research in Fluid Mechanics and Thermal Sciences*, 63, 260-273.

[3] Sahel, D., Ameur, H., Benzeguir, R., Kamla, Y. (2018). Prediction of heat transfer development in a smooth tube. *Journal of Engineering Physics and Thermophysics*, 91, 682-687.

[4] Ozsipahi, M., Subasi, A., Gunes, H., Sahin, B. (2018). Numerical investigation of hydraulic and thermal performance of a honeycomb heat sink. *International Journal of Thermal Sciences*, 134, 500-506.

[5] Haghighi, S. S., Goshayeshi, H. R., Safaei, M. R. (2018). Natural convection heat transfer enhancement in new designs of plate-fin based heat sinks. *International Journal of Heat and Mass Transfer*, 125, 640-647.

[6] Sahel, D., Ameur, H., Benzeguir, R., Kamla, Y. (2016). Enhancement of heat transfer in a rectangular channel with perforated baffles. *Applied Thermal Engineering*, 101, 156-164.

[7] Meinders, E. R., Van Der Meer, T. H., Hanjalic, K. (1998). Local convective heat transfer from an array of wall-mounted cubes. *International Journal of Heat and Mass Transfer*, 41, 335-346.

[8] Sara, O. N., Pekdemir, T., Yapici, S. İ. N. A. N., Yilmaz, M. (2001). Heat-transfer enhancement in a channel flow with perforated rectangular blocks. *International Journal of Heat and Fluid Flow*, 22, 509-518.

[9] Huang, C. H., Liu, Y. C., Ay, H. (2015). The design of optimum perforation diameters for pin fin array for heat transfer enhancement. *International Journal of Heat and Mass Transfer*, 84, 752-765.

[10] Chin, S. B., Foo, J. J., Lai, Y. L., Yong, T. K. K. (2013). Forced convective heat transfer enhancement with perforated pin fins. *Heat and Mass Transfer*, 49(10), 1447-1458.

[11] Sahel, D., & Benzeguir, R. (2017). Thermal characteristic in solar air heater fitted with plate baffles and heating corrugated surface. *Energy Procedia*, 139, 307-314.

[12] Sahel, D., Benzeguir, R., Baki, T. (2015). Heat transfer enhancement in a fin and tube heat exchanger with isosceles vortex generators. *Mechanika*, 21(6), 457-464.

[13] Sahel, D. (2021). Thermal performance assessment of a tubular heat exchanger fitted with flower baffles. *Journal of Thermophysics and Heat Transfer*, 35(4), 726-734.